Nanowire Plasmon Excitation by Adiabatic Mode Transformation

Ewold Verhagen,* Marko Spasenović, Albert Polman, and L. (Kobus) Kuipers

Center for Nanophotonics, FOM Institute for Atomic and Molecular Physics (AMOLF), Science Park 113, 1098 XG, Amsterdam, The Netherlands

(Received 6 February 2009; revised manuscript received 20 April 2009; published 19 May 2009)

We show with both experiment and calculation that highly confined surface plasmon polaritons can be efficiently excited on metallic nanowires through the process of mode transformation. One specific mode in a metallic waveguide is identified that adiabatically transforms to the confined nanowire mode as the waveguide width is reduced. Phase- and polarization-sensitive near-field investigation reveals the characteristic antisymmetric polarization nature of the mode and explains the coupling mechanism.

DOI: 10.1103/PhysRevLett.102.203904 PACS numbers: 42.82.Et, 68.37.Uv, 73.20.Mf, 78.66.Bz

Surface plasmon polaritons (SPPs) are electromagnetic waves coupled to charge oscillations at a metal-dielectric interface. Their combined nature as part matter excitation and part light field enables strong control of electromagnetic fields at subwavelength length scales. Metal surfaces support evanescent waves for all frequencies smaller than the surface plasmon resonance frequency. Whereas in all-dielectric photonic structures the wavelength in the dielectric sets a lower bound to the size to which light can be confined, properly shaped metallic structures can confine light fields to arbitrarily small length scales. The potential of highly confined SPPs includes subwavelength guiding [1–8], efficient single-molecule sensing [9], enhanced nonlinear effects [10–12], and the miniaturization of photonic circuits [1,2,13]. Moreover, the small mode sizes of nanoscopic plasmon waveguides lead to a strong interaction with individual quantum emitters, which may be useful in quantum information [14–16]. On a metallic cylinder a waveguided mode with azimuthal field symmetry, i.e., having "radial" polarization, exists for any cylinder radius. At terahertz frequencies and below, these so-called Sommerfeld waves are, in general, only weakly guided [17,18]. In the optical and near-infrared regime, however, the analogous SPP wave propagating along a metal nanowire is predicted to become strongly confined to the wire when its radius is reduced to tens of nanometers [5,19–22]. The combination of the subwavelength mode profile and the radial symmetry of the nanowire mode causes the field overlap integral of this mode with a linearly polarized light wave to be very small. This makes it difficult to couple the nanowire mode efficiently to or from a macroscopic wave, such as a beam incident from the far field or a low-loss guided mode in a typical wavelength-sized waveguide.

In this work, we identify a unique SPP mode propagating on a metallic stripe of micron-scale width, which continuously evolves to the nanowire mode as the width of the stripe is decreased. When this mode is excited in a stripe that is tapered down to the desired nanowire size, the wave propagating along the taper can remain in the corresponding eigenmode, thereby being adiabatically converted to the nanowire mode. We experimentally demonstrate that such a structure can thus serve as the required coupling element to efficiently excite nanowire SPPs. The transformation and subsequent propagation of SPPs on nanowires as small as 60 nm is investigated by near-field microscopy. By combining phase and polarization sensitivity, we experimentally reveal the special polarization nature of the excited nanowire mode, underpin the efficiency of the adiabatic transformation process, and determine the dispersion and losses of the nanowire mode.

Figure 1 explains the mode transformation mechanism. It presents the calculated width dependence of the normalized wave vector $\Re\{k_\parallel\}/k_0$ of the modes guided by a 77 nm thick straight Au stripe on glass for various wavelengths, where $k_\parallel$ is the SPP wave vector component along the waveguide and $k_0 = \omega/c$ is the free-space wave vector.

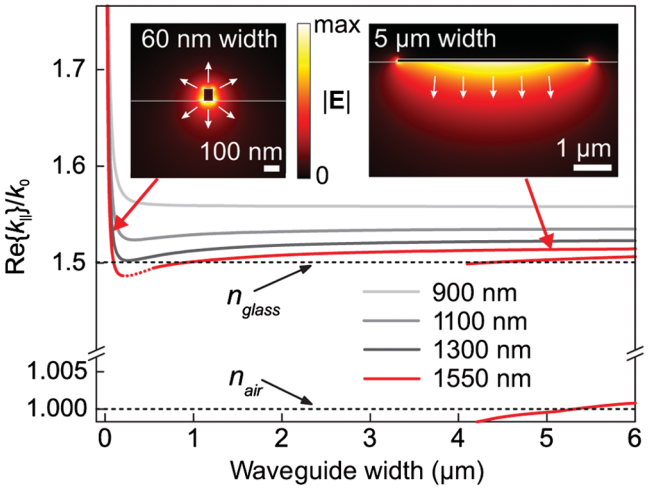

FIG. 1 (color). Normalized wave vector of the SPP modes guided by a Au waveguide on glass as a function of waveguide width. The dots between 200 and 550 nm widths for 1550 nm are a cubic spline interpolation [23]. For shorter wavelengths, only the fundamental mode is indicated. Plotted also are the cross sections of the electric field amplitude of the fundamental mode for 60 nm and 5 μm widths at a free-space wavelength of 1550 nm. The arrows schematically depict the direction of the transverse electric field.

The calculations are performed with a finite element mode solver using perfectly matched layer boundary conditions [23]. For large widths the asymmetry of the dielectric environment has a strong effect on eigenmodes of the waveguide, separating modes that are localized predominantly in air (with $\Re\{k_\parallel\}/k_0 \approx 1$) or in glass ($\Re\{k_\parallel\}/k_0 \approx 1.5$) [24,25]. When the width is reduced, only one mode persists. It exhibits a diverging wave vector, characteristic for highly confined plasmonic modes. If the waveguide size of dielectric or photonic crystal waveguides decreases, the wave vector either decreases until guided propagation stops at the critical waveguide cutoff size, or it asymptotically approaches the wave vector in the surrounding medium, in conjunction with a continuously increasing extent of the evanescent field outside the waveguide. The latter is also the case for long-range SPP waves observed to propagate along nanowires in a homogeneous dielectric environment [23,26,27]. In contrast, the mode considered here is confined in a subwavelength area around the nanowire for small widths. It can be recognized as the nanowire mode, the rectangular equivalent of the Sommerfeld wave in a metal cylinder in a homogeneous environment. Like that wave, the transverse electric field at opposite sides of the waveguide has opposite sign. This polarization nature, from here on called "antisymmetric," is related to surface charges having equal sign around the circumference of the nanowire. As a result, the field interferes constructively inside the metal, giving rise to large induced charges and a pronounced longitudinal electric field component. For longer wavelengths, the wave vector is first slightly reduced when the waveguide narrows, as the fraction of the modal field guided in air increases through the mode transformation. Importantly, the field of the mode of interest (which has the lowest energy) is predominantly localized at the substrate side of the guide for large widths. This mode is responsible for the focusing of SPPs on the substrate side of a laterally tapered metal film [28]. Air-guided modes, which have previously been used to excite waveguides of subwavelength width [29,30], are unsuitable for adiabatic coupling to the nanowire mode [23]. This is clear in Fig. 1 from the fact that the normalized wave vector of these modes crosses the substrate light line as the width of the metal stripe is decreased. The broken symmetry in the system described in this work is responsible for the broad, Gaussian-like mode profile and approximately linear polarization at large widths, which enables a more straightforward excitation of the required mode that is to be transformed. In contrast, the corresponding mode on a stripe embedded in a homogeneous dielectric environment would be localized at the waveguide edges, while having a purely antisymmetric field distribution [23,31].

In the experiment the desired mode on the substrate side of a Au film on BK7 glass is excited at the entrance of a 5 μm wide waveguide with 1550 nm light using a hole array made in the 77 nm thick Au film with a 1 μm pitch [23]. An optical microscope image of the structure is shown in Fig. 2(a). The width of the waveguide decreases over a length of 20 μm after which the waveguide connects to a nanowire. The evanescent SPP field is probed above the sample with a phase-sensitive near-field microscope which yields both the local field amplitude $|A|$ and the phase ϕ [32]. The complex signal $A = |A|e^{i\phi}$ is a projection of the vectorial near field on the polarization state in the reference beam [33].

Figure 2(b) shows a map of the measured near-field amplitude $|A|$. In the left part of the image, the hole array with which the SPPs are excited is visible. In the tapered section, the presence of SPPs propagating at the Au-glass interface is evidenced only by a field amplitude along the edge of the waveguide, as for these widths almost all of the energy of the SPP mode is located below the Au. At the end of the taper, the SPPs couple to a 150 nm wide nanowire. Near the end of the taper, a clear intensity increase is observed as the guided wave becomes more strongly con-

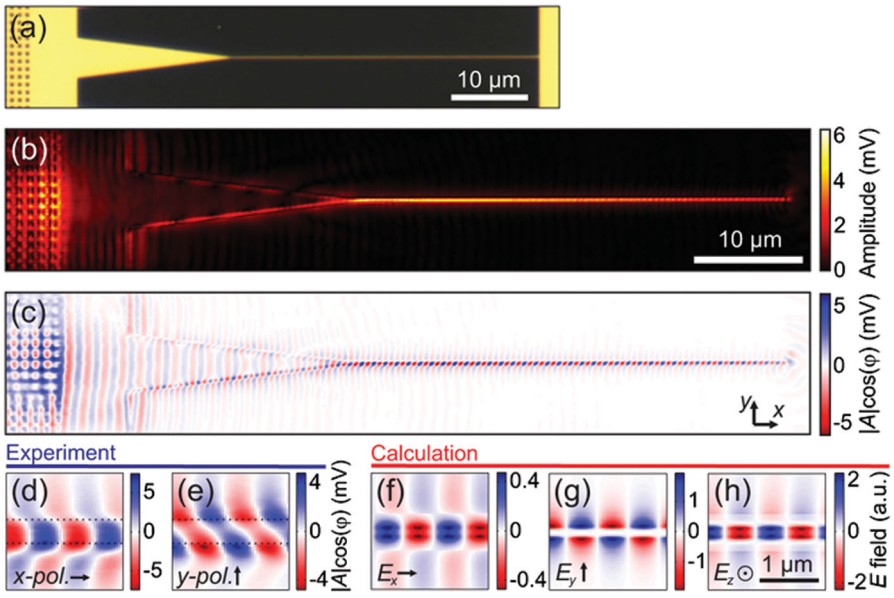

FIG. 2 (color). Near-field imaging of SPP excitation and propagation on a nanowire. (a) Optical microscope image of the structure. (b) Collected near-field SPP amplitude and (c) distribution of $|A|\cos\phi$. SPPs excited on the Au-glass surface in the left are converted to a mode guided along a 150 nm wide nanowire. The excitation wavelength is 1550 nm. (d),(e) Measured $|A|\cos\phi$ on a small section of the nanowire for x and y polarizations. The dotted lines indicate the height step that the near-field probe makes due to the presence of the nanowire. (f)–(h) Calculated field components E_x, E_y, and E_z at a height of 20 nm above the sample.

centrated and the fraction of the modal field in air increases at the same time. The absence of phase or wavelength changes along the edges of the taper in the distribution of $|A|\cos\phi$ depicted in Fig. 2(c) shows that indeed the SPPs guided along the substrate side of the film smoothly convert to the nanowire SPP. The SPP wave is guided along the 40 μm long wire until the wire terminates in a continuous Au film. The full width at half maximum of the intensity in the guided beam is 300 nm, which constitutes only an upper limit to the mode size as the probe diameter was 220 nm. The transverse size of the guided mode is therefore considerably smaller than the 1550 nm free-space wavelength, experimentally proving that this structure can lead to nanofocusing of SPPs [20] and subsequent subwavelength guiding.

To investigate the nature of the excited nanowire mode, we vary the polarization of the reference beam, effectively selecting a polarization in the signal branch. Because the components of the optical near field couple to orthogonal polarizations in the probe fiber in different ways, this technique yields information about the vectorial character of the near field [23,33]. Orthogonal polarization angles can be found for which in-plane electric near-field components along either x or y contribute predominantly to the detected signal. Figures 2(d) and 2(e) show spatial profiles of $|A|\cos\phi$ measured on a small section of the nanowire for these two polarization angles. The measured signal distribution obtained with the polarization corresponding to the x direction (longitudinal to the wire) is highly symmetric with respect to the center of the wire, whereas the y polarization (transverse to the wire) is largely antisymmetric.

The observed symmetries are intimately related to the symmetry of the nanowire mode. The calculated electric field components of the mode are depicted in Figs. 2(f)–2(h), for the height contour that the near-field probe follows. The measured pattern for x polarization [Fig. 2(d)] closely resembles that of the calculated longitudinal field E_x. The close resemblance indicates that E_x provides the dominant contribution to the symmetric image, rather than the out-of-plane component E_z, which is also symmetric but with flat wave fronts unlike both E_x and the measured pattern. The measured amplitude of the longitudinal x polarization is comparable to that of the measured antisymmetric transverse y polarization [compare the amplitudes in Figs. 2(d) and 2(e)]. The presence of a significant longitudinal field demonstrates the pronounced deviation of the highly confined nanowire mode from a transverse wave. It is immediately connected to the strong transverse confinement of the nanowire mode since $\partial E_y/\partial y + \partial E_z/\partial z = -ik_x E_x$, following from Coulomb's law. The observed antisymmetric distribution for y polarization [Fig. 2(e)] is related to the E_y field component. It proves that the excited nanowire mode is antisymmetric, like a Sommerfeld wave.

From the phase evolution of the mode, its wave vector is determined. Figure 3(a) shows measured dispersion curves for nanowire widths of 60, 85, and 150 nm, obtained by varying the excitation laser wavelength between 1450 and 1570 nm in 2 nm steps. As expected (see Fig. 1), for a given frequency the largest wave vector is observed for modes on the narrowest nanowire. The wave vector is in all cases close to that of light in the substrate, even though a significant fraction of the optical energy is guided in air. The plasmonic nature of the mode is clearly recognizable by the significantly reduced group velocity $d\omega/dk$, which is determined to be $0.83c/n_{\mathrm{glass}}$ for the 60 nm wide nanowire from a linear fit to the data. The measured normalized wave vector and propagation lengths ($L = \frac{1}{2}\Im\{k_\parallel\}^{-1}$, obtained from exponential fits to the near-field maps) are compared to theory for a free-space wavelength of 1550 nm in Fig. 3(b). For the two smallest widths, excellent agreement is found between measurements and calculations, which contain no adjustable parameters. The origin of the deviation for the 150 nm wide waveguide is as yet unknown; it indicates that the leakage into the substrate (which occurs for $\Re\{k_\parallel\}/k_0 < n_{\mathrm{glass}}$) is larger than calculated. The excellent agreement between the measured and

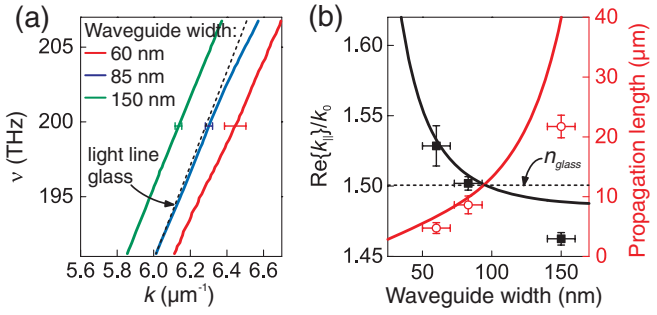

FIG. 3 (color). (a) Measured dispersion curves for three Au nanowire widths. The dashed line denotes the dispersion of light in the substrate. The error bars represent the experimental uncertainty. (b) Measured wave vector and propagation length as a function of waveguide width (symbols), compared to calculations (curves) for a free-space wavelength of 1550 nm.

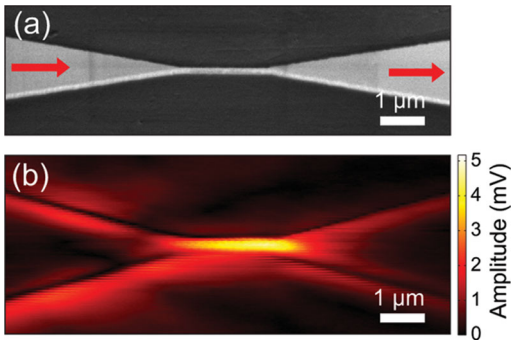

FIG. 4 (color). (a) Secondary electron micrograph of a 2 μm long nanowire connected by tapered waveguide sections for input and output coupling. (b) Near-field amplitude of forward-propagating waves in the structure at $\lambda = 1550$ nm. The intensity transmission of the complete structure is $20 \pm 6\%$.

calculated propagation lengths for small widths indicates that Ohmic dissipation is the dominant loss mechanism, since the calculations neglect scattering losses.

To demonstrate that the adiabatic mode transformation causes an efficient transition to the nanowire, we consider a structure consisting of two tapers connected by a 2 μm long nanowire [Fig. 4(a)]. SPPs incident from the left are converted from a waveguide width of 2 μm to a 90 nm wide nanowire. In the output taper on the right, the transmitted SPPs are converted back to a 2 μm width. Figure 4(b) shows the near-field amplitude of waves that propagate from left to right, obtained from the experimental data using a Fourier analysis [34]. By comparing the amplitudes at the edges of the taper at 4 μm distance to either side of the nanowire, we determine the total intensity transmission to be $20 \pm 6\%$. From the Fourier analysis, a $2 \pm 1\%$ backreflection loss is found. By correcting for the known propagation loss of the 2 μm long nanowire [Fig. 3(b)], the combined coupling and decoupling efficiency of both tapers is calculated to be $I_{\mathrm{in}} e^{-l/L}/I_{\mathrm{out}} = 24 \pm 7\%$, with l the nanowire length. This corresponds to an average loss of $\sim$50% per coupler. This is in good agreement with calculations and comparable to that which would be expected in a cylindrical geometry [23]. The loss includes dissipation in the tapers, scattering to free-space radiation, and leakage of the mode into the substrate when $\Re\{k_{\|}\}/k_0 < n_{\mathrm{glass}}$. Many parameters can be identified to improve the efficiency: The use of Ag rather than Au will reduce Ohmic damping, leakage radiation can be eliminated by increasing the refractive index of the substrate or reducing the film thickness, and an optimal tapering profile can further optimize adiabaticity and taper length. The optimum efficiency will be obtained by balancing Ohmic and scattering losses. A rough estimate of a lower bound to the maximum possible efficiency of $\sim$70% is obtained by assuming that the dissipative loss in the complete length of the taper is equal to that in the nanowire. This is, however, a conservative estimate, since the absorption in most of the taper is much lower than in the narrow nanowire.

In conclusion, we have shown the excitation of highly confined nanowire SPPs through the principle of adiabatic mode transformation. We have presented new calculations that identify a specific mode that can transform to a subwavelength-scale nanowire mode bearing strong resemblance to a Sommerfeld wave, while being easily excitable in a wide metallic waveguide. Phase- and polarization-sensitive near-field microscopy revealed the characteristic antisymmetric polarization nature of the excited nanowire mode and showed that it gradually and efficiently evolves from the fundamental SPP mode propagating at the substrate side of a metal stripe waveguide. These results demonstrate a practical implementation of the nanoscale miniaturization of light on a chip and provide the necessary tools to interface the macroscopic world with individual nano-objects.

This work is part of the research program of FOM, which is financially supported by NWO. It is further supported by the EC-funded project PhOREMOST (FP6/2003/IST/2-511616), NANONED, and by the Joint Solar Program (JSP) of FOM, which is cofinanced by gebied Chemische Wetenschappen of NWO and Stichting Shell Research. M. S. acknowledges the support of the European Community under the Marie Curie Scheme (Contract No. MEST-CT-2005-021000). The authors thank Matteo Burresi, Dries van Oosten, and Tobias Kampfrath for useful discussions.

*verhagen@amolf.nl

[1] S. I. Bozhevolnyi *et al.*, Nature (London) **440**, 508 (2006).
[2] J. A. Dionne, H. J. Lezec, and H. A. Atwater, Nano Lett. **6**, 1928 (2006).
[3] M. Quinten *et al.*, Opt. Lett. **23**, 1331 (1998).
[4] S. A. Maier *et al.*, Nature Mater. **2**, 229 (2003).
[5] J. Takahara *et al.*, Opt. Lett. **22**, 475 (1997).
[6] R. M. Dickson and L. A. Lyon, J. Phys. Chem. B **104**, 6095 (2000).
[7] H. Ditlbacher *et al.*, Phys. Rev. Lett. **95**, 257403 (2005).
[8] M. W. Knight *et al.*, Nano Lett. **7**, 2346 (2007).
[9] S. Nie and S. R. Emory, Science **275**, 1102 (1997).
[10] A. Bouhelier *et al.*, Phys. Rev. Lett. **90**, 013903 (2003).
[11] J. A. H. van Nieuwstadt *et al.*, Phys. Rev. Lett. **97**, 146102 (2006).
[12] S. Kim *et al.*, Nature (London) **453**, 757 (2008).
[13] T. W. Ebbesen, C. Genet, and S. I. Bozhevolnyi, Phys. Today **61**, No. 5, 44 (2008).
[14] D. E. Chang *et al.*, Phys. Rev. Lett. **97**, 053002 (2006).
[15] D. E. Chang *et al.*, Nature Phys. **3**, 807 (2007).
[16] A. V. Akimov *et al.*, Nature (London) **450**, 402 (2007).
[17] A. Sommerfeld, Ann. Phys. (Berlin) **303**, 233 (1899).
[18] K. Wang and D. M. Mittleman, Nature (London) **432**, 376 (2004).
[19] A. J. Babadjanyan, N. L. Margaryan, and K. V. Nerkararyan, J. Appl. Phys. **87**, 3785 (2000).
[20] M. I. Stockman, Phys. Rev. Lett. **93**, 137404 (2004).
[21] L. Novotny, Phys. Rev. Lett. **98**, 266802 (2007).
[22] U. Schröter and A. Dereux, Phys. Rev. B **64**, 125420 (2001).
[23] See EPAPS Document No. E-PRLTAO-102-056922 for supplementary information providing a detailed discussion of the experimental and computational techniques used. For more information on EPAPS, see http://www.aip.org/pubservs/epaps.html.
[24] J.-C. Weeber *et al.*, Phys. Rev. B **64**, 045411 (2001).
[25] R. Zia, M. D. Selker, and M. L. Brongersma, Phys. Rev. B **71**, 165431 (2005).
[26] K. Leosson *et al.*, Opt. Express **14**, 314 (2006).
[27] J. Jung, T. Søndergaard, and S. I. Bozhevolnyi, Phys. Rev. B **76**, 035434 (2007).
[28] E. Verhagen *et al.*, Opt. Express **16**, 45 (2008).
[29] L. Yin *et al.*, Nano Lett. **5**, 1399 (2005).
[30] J. R. Krenn *et al.*, Europhys. Lett. **60**, 663 (2002).
[31] P. Berini, Phys. Rev. B **61**, 10 484 (2000).
[32] M. L. M. Balistreri *et al.*, Phys. Rev. Lett. **85**, 294 (2000).
[33] M. Burresi *et al.*, Phys. Rev. Lett. **102**, 033902 (2009).
[34] R. J. P. Engelen *et al.*, Nature Phys. **3**, 401 (2007).